Rev. Roum. Sci. Techn.– Électrotechn. et Énerg.
Vol. **67**, *2*, pp. 117–122, Bucarest, 2022

OPTIMAL REACTIVE POWER MANAGEMENT FOR MICROGRIDS BASED ON PHOTOVOLTAIC INVERTERS USING SINE-COSINE ALGORITHM

MIHAI BURLACU, VALENTIN NĂVRĂPESCU, AUREL IONUȚ CHIRILĂ, IOAN DRAGOȘ DEACONU

Keywords: Photovoltaic; Inverters; Sine cosine algorithm; Microgrid; Optimal reactive power management.

In this paper, an optimization problem is formulated for determining the optimal reactive power management strategy, for a microgrid, based on the reactive power support provided by the inverters from photovoltaic power plants (PVPPs). The optimization problem is solved by applying a recent and performant metaheuristic, namely the sine-cosine algorithm. Multiple scenarios are defined, depending on the load and PVPP active power output, and the results obtained by the proposed strategy are presented in comparison with a reactive power management strategy based only on capacitor banks (CBs).

1. INTRODUCTION

In recent times, policymakers worldwide are increasing their efforts for mitigating climate change. The current measures enforced for all economic sectors are also imposing new challenges on power systems. In this context, the integration of high penetration renewable energy sources represents one of the most important measures, appliable to power systems, for reducing the global CO_2 footprint. Renewable energy sources are currently integrated into all sectors of power systems, from small-scale residential or commercial applications up to utility-scale power plants, as most economic systems have supported the investors by introducing various incentives. Consequently, wind and solar are the most popular renewable energy sources that have seen spectacular development in recent years. As the main disadvantages of high upfront costs and large necessary surfaces were successfully compensated by introducing various incentives, PVs made remarkable progress, also sustained by their advantages such as scalability, as PVs have applications from a few W or kW (such as telephone chargers and residential PV arrays) up to tens of MW at utility-scale PVPPs, low maintenance cost, very low operational costs, and relatively long-life cycles. As a result, solar energy generated worldwide has increased from 3350 TWh in 2014 up to 40770 TWh in 2020 [1], which represents a 12-time increase in six years. Although, there is still a long road toward zero-emissions power systems, during the last decade a change of paradigm has already been observed in the energy sector.

A natural consequence of integrating renewable energy sources is that power systems are transitioning towards a more decentralized operation model, which requires new technologies for improving the efficiency of small groups comprising controllable loads, distributed generation sources, and storage devices. In recent years, microgrids are increasing in popularity and are evolving towards a regular presence in power systems, rather than an experimental proof-of-work for a theoretical concept. As defined by [2], a microgrid is "a group of interconnected loads and distributed energy resources with clearly defined electrical boundaries that act as a single controllable entity with respect to the grid and can connect and disconnect from the grid to enable it to operate in both grid-connected and island modes".

Digitalization represents one of the key factors for assuring microgrids' controllability, as data from all controllable entities need to be collected and transmitted to the local controller. In turn, the local controller requires performant hardware resources and efficient software algorithms to make the decisions and transmit them back to the controllable entities to assure the optimal microgrid operation. Both classical methods and metaheuristic algorithms are applied for solving a large variety of optimization problems formulated for microgrid operation, scheduling, and planning. The research literature shows during the recent period that metaheuristic algorithms are currently a very popular choice for solving various medium-sized optimization problems, as they provide accurate results without employing additional complex mathematical models. The authors of [3] proposed an optimal microgrid energy management strategy by using An Asynchronous Decentralized Particle Swarm Optimizer, while in [4] a power management enhancement strategy is determined by using an adaptive Ant Lion Optimizer. Another microgrid optimal energy management strategy is determined in [5] by using a grey wolf optimizer, alongside the optimal battery energy storage system sizing. An optimal BESS scheduling strategy for a microgrid is also provided in [6], by using a genetic algorithm. In [7] the authors apply a Multi-Objective Hunger Game Search Optimizer for finding the optimal BESS scheduling strategy for a grid-connected microgrid, while [8] presents a power quality enhancement in autonomous microgrids based on a Particle Swarm Optimizer. Furthermore, metaheuristic algorithms applications are not limited to microgrids, as numerous studies are also conducted on distribution and transmission grids. For example, in [9], an optimal BESS scheduling strategy is determined by using a Mutation-Improved Grey Wolf Optimizer upon distribution network characterized by high renewable energy sources penetration. Paper [10] proposes an improvement for solving optimal power flow salp swarm algorithm problems for transmission networks and [11] presents a unit commitment optimization based on an improved genetic algorithm. Metaheuristic solvers are also applied in designing and tunning controllers for power systems. For example, in [12], a Non-Dominated Sorting Genetic Algorithm is applied for the optimal tuning of a power system stabilizer, while [13] proposes a direct power control for a doubly fed induction generator based on an adaptive neural fuzzy sliding controller optimized by genetic algorithm.

This paper applies the sine-cosine algorithm for

University „Politehnica" of Bucharest, Electrical Engineering Faculty, mvbcad@gmail.com

determining the optimal reactive power management strategy for a microgrid, using the reactive power generated by the PVPPs inverters. The paper is organized as follows. The first section is the introduction, section 2 presents the mathematical model. The sine-cosine algorithm is described in section 3, while section 4 presents the case study.

2. MATHEMATICAL MODEL

2.1. THE OBJECTIVE FUNCTION

The reactive power management problem formulated in this study aims to minimize the microgrid total active power losses ΔP_{total}, as follows:

$$\begin{aligned} &\min f(x) = \Delta P_{total}, \\ &\text{subject to}: \begin{matrix} g(x) = 0, \\ h(x) \le 0, \end{matrix} \end{aligned} \tag{1}$$

where f is the objective function, x is the vector of control variables, g is the equality constraints, and h is the inequality constraints.

The control variables vector x consists of the PVPPs reactive power output $Q_{g,1}$ … $Q_{g,N}$ and the capacitor banks operating step $n_{CB,1}$ … $n_{CB,n}$:

$$x = [Q_{g,1}...Q_{g,N}, n_{CB,1}...n_{CB,n}]. \tag{2}$$

The total active power losses are determined based on the microgrid active power balance, as the difference between the total active power supplied to the microgrid (by the up-stream sub-station P_{slack} and PVPPs $P_{g,i}$) and the total power demanded by the loads ($P_{C,i}$):

$$\Delta P_{total} = P_{slack} + \sum_{i=1}^{N} P_{g,i} - \sum_{i=1}^{n_b} P_{C,i} \tag{3}$$

2.2. EQUALITY AND INEQUALITY CONSTRAINTS

The equality constraints $g(x)$ from (1) are used for performing the load flow calculation and consist of the nodal active and reactive power equations [14]:

$$\begin{aligned} P_i - \sum_{k=1}^{n_B} U_i U_k \left[G_{ik} \cos(\theta_i - \theta_k) + B_{ik} \sin(\theta_i - \theta_k) \right] = 0, \\ Q_i + \sum_{k=1}^{n_B} U_i U_k \left[B_{ik} \cos(\theta_i - \theta_k) - G_{ik} \sin(\theta_i - \theta_k) \right] = 0, \end{aligned} \tag{4}$$

where P_i and Q_i are the nodal active and reactive powers, U_i, U_k and θ_i, θ_k are the voltage amplitudes and angles at buses i and k, while G_{ik} and B_{ik} are the real and imaginary part of the i-k term from the bus admittance matrix.

The inequality constraints $h(x)$ is given in eqs. (5) – (8). The first two inequality constraints represent the operational constraints for the PVPP inverters reactive power output and capacitor banks operating steps and are given below:

$$Q_{g,i}^{min} \le Q_{g,i} \le Q_{g,i}^{max}, \tag{5}$$

$$n_{CB,i}^{min} \le n_{CB,i} \le n_{CB,i}^{max}, \tag{6}$$

where $Q_{g,i}^{min}$ and $Q_{g,i}^{max}$ are the i^{th} PVPP reactive power limits, while $n_{CB,i}^{min}$ and $n_{CB,i}^{max}$ represent the minimum and maximum operating step for the i^{th} capacitor bank.

The inverter minimum and maximum reactive power limits can be set considering the power factor and the active power output or depending on the inverter's apparent power limit [15]. In this study, the reactive power limits are determined at the rated active power and minimum power factor and considered constant for all active power output values from 0 % to 100 %.

The other two inequality constraints consisting in the microgrid operational constraints regarding the bus voltages and branch currents are presented below:

$$V_i^{min} \le V_i \le V_i^{max}, \quad \forall i = 1...n_B, \tag{7}$$

$$|I_i| \le I_i^{max}, \quad \forall i = 1...n_L, \tag{8}$$

where V_i^{min} and V_i^{max} are the lower and upper admissible voltage values for bus i, I_i^{max} is the admissible current through branch i, while n_B and n_L are the numbers of microgrid buses and lines.

2.3. ADAPTATIONS FOR METAHEURISTIC SOLVERS

A meta-heuristic algorithm, namely the Sine-Cosine Algorithm (presented in section 3), is applied in this study for solving the optimization problem, therefore several adaptations are introduced to assure that the equality and inequality constraints are satisfied.

The first adaptation consists in performing the load flow calculation, by using the backward-forward sweep (BFS) method, to assure that the equality constraints $g(x)$ from (1) are satisfied. The BFS method is the most appropriate as the study is focused upon an MV microgrid, characterized by a radial or tree-like topology and low X/R ratio. Firstly, a preprocessing stage, based on the graph theory, is necessary to determine the graph which models the microgrid topology, the predecessor and successors for each bus, and the order in which buses are visited. Within the BFS method, the loads and distributed energy sources are modeled as constant active and reactive powers absorbed/injected at the buses, while the capacitor banks are modeled as constant shunt impedances.

The BFS is an iterative method, which begins by initializing all bus voltages with the voltage value at the slack bus. Each iteration consists of two main stages: (1) the backward sweep, when the currents demanded by the loads and the currents through the network branches are determined, and (2) the forward sweep, when the voltage drops across the branches and bus voltages are computed. After each iteration, the complex apparent power supplied by the slack bus is computed and a convergence test is performed to decide if a new iteration is performed, or the iterative process has reached the results.

The inequality constraints (5) and (6) regarding the PVPP reactive power limits and CB step limits are imposed as lower and upper bounds for the decision variables $Q_{g,i}$ and $n_{CB,i}$. The inequality constraints regarding the microgrid operational constraints are introduced as penalty functions. Consequently, the penalized objective function F is defined as the sum between the objective function f and the penalty functions P_1 and P_2.

$$F(x) = f(x) \cdot \alpha + P_1 + P_2 . \quad (9)$$

The divergent load flow solutions will be penalized by applying the additional penalty coefficient (α) to multiply objective function by a large value, while for the convergent solutions, α = 1.

Penalty function P_1 is applied to enforce constraint (7) regarding the voltage limits. P_1 is defined as the sum between the penalty coefficients $p_{1,i}$, which are zero only if the i^{th} bus voltage is within admissible limits.

$$P_1 = \sum_{i=1}^{n_B} p_{1,i} , \quad (10)$$

$$p_{1,i} = \begin{cases} (U_{min,i} - U_i), & \text{if } U_i < U_{min,i}, \\ 0, & \text{if } U_{min,i} \le U_i \le U_{max,i}, \\ (U_i - U_{max,i}), & \text{if } U_i > U_{max,i}. \end{cases} \quad (11)$$

The second penalty function P_2 is defined as the sum between the penalty coefficients $p_{2,i}$, which are zero if the i^{th} branch current is within the admissible limit.

$$P_2 = \sum_{i=1}^{n_L} p_{2,i} , \quad (12)$$

$$p_{2,i} = \begin{cases} 0, & \text{if } I_i \le I_{max,i}, \\ (I_i - I_{max,i}), & \text{if } I_i > I_{max,i}. \end{cases} \quad (13)$$

3. SINE-COSINE ALGORITHM

The Sine-Cosine Algorithm is a relatively recent metaheuristic algorithm, proposed by S. Mirjalili in 2016, [16]. Given its simplicity and increased performance, the SCA has become a very popular metaheuristic algorithm, applied in a significant number of research papers, in its original form or in various modified, hybridized, and multi-objective versions [17]. SCA is also applied in solving power system optimization problems, such as economic and emission dispatch [18], optimal tuning of a PID controller for a solar system [19], optimal allocation of distributed energy sources [20], *etc*.

The SCA is a highly-performant and robust optimizer, with the major advantage of having a straightforward algorithm, which basically consists of one mathematical expression and several random numbers for updating the candidate solutions. The position updating mechanism is based upon the trigonometric sine and cosine functions, as presented below:

$$X_i^{t+1} = \begin{cases} X_i^t + r_1 \times \sin(r_2) \times \left| r_3 \cdot P_i^t - X_i^t \right|, \text{for } r_4 < 0.5, \\ X_i^t + r_1 \times \cos(r_2) \times \left| r_3 \cdot P_i^t - X_i^t \right|, \text{for } r_4 \ge 0.5, \end{cases} \quad (14)$$

where X_i^t represents the position in the i^{th} dimension of a candidate solution at iteration t, P_i^t is the position in the i^{th} dimension of the best solution discovered at iteration t, while r_1, r_2, r_3 and r_4 are random numbers.

As (14) reveals, the SCA is based on four parameters: r_1, r_2, r_3 and r_4. The first parameter, r_1 is used to decide if the candidate solution is heading towards ($r_1 < 1$) or outwards ($r_1 > 1$) as the best solution. Therefore, the balance between exploitation and exploration is maintained by linearly decreasing r_1 starting from a constant a to 0, as the current iteration t advances towards the maximum iteration T:

$$r_1 = a - t\frac{a}{T} . \quad (15)$$

Parameter r_2 is applied for defining how far the candidate solution moves towards or outwards from the destination. As r_2 is the argument of the sine and cosine function, it is set in the [0, 2π] range. The third parameter r_3 is used for emphasizing ($r_3 > 1$) or deemphasizing ($r_3 < 1$) the destitution's contribution in choosing the next position, while r_4 is simply a switch for choosing between the sine and cosine functions. Finally, the position update mechanism is illustrated in Fig. 1.

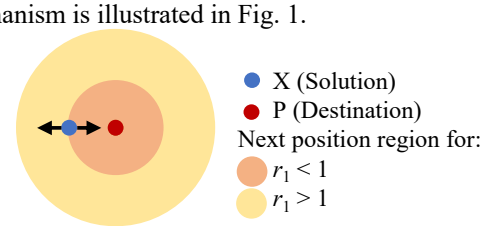

Fig. 1 – The position update mechanism for the sine-cosine algorithm.

The SCA pseudo-code, presented below reveals its remarkable simplicity, as only one mechanism is applied for updating the positions:

Initialize a set of solutions X
while t is less than T do
  Evaluate the objective function for each solution X
  Update the destination P (the best solution so far)
  Generate the random parameters r_1, r_2, r_3 and r_4
  Update solution X using (10)
end while
Return the destination P.

4. CASE STUDY

4.1 THE MICROGRID UNDER STUDY

The case study presented in this paper is conducted on a 20 kV grid-connected microgrid, which supplies seven loads through seven MV underground electrical lines, from the MV busbar of a step-down substation. Also, the microgrid comprises four PVPPs and three capacitor banks. The microgrid one-line diagram is presented in Fig. 2. It should be mentioned that the tree-like topology, with one main axis and one derivation, is inspired by the European version of the CIGRE MV benchmark network introduced in [21].

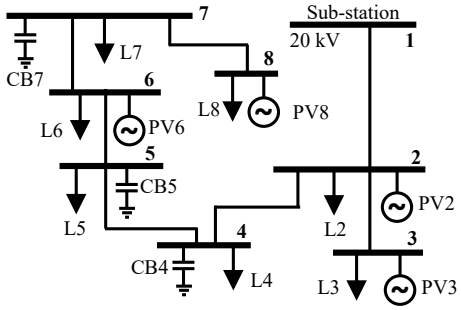

Fig. 2 – Microgrid one-line diagram.

The active (P_i) and reactive (Q_i) power demanded by

each of the seven loads, alongside the corresponding apparent power (S_i) and power factor ($\cos\varphi_i$) are presented in Table 1, for the base load scenario.

Table 1

Load data

Load	P_i [kW]	Q_i [kvar]	S_i [kVA]	$\cos\varphi_i$ [–]
L2	255	155	298.4	0.855
L3	705	475	850.1	0.829
L4	465	310	558.9	0.832
L5	425	245	490.6	0.866
L6	335	165	373.4	0.897
L7	535	330	628.6	0.851
L8	765	485	905.8	0.845

Table 2 shows the electrical lines' parameters: resistance (r_0), reactance (x_0), susceptance (b_0), rated current (I_{max}) and power (S_{max}), extracted from [22], alongside the line length.

Table 2

Electrical lines data

Line	Length [km]	Parameters
L12	3.25	r_0 = 0.927 Ω/km x_0 = 0.142 Ω/km b_0 = 47.12389 μS/km I_{max} = 150 A S_{max} = 5196.2 kVA
L23	0.90	
L24	0.85	
L45	0.75	
L56	0.55	
L67	0.75	
L78	0.60	

As mentioned before, the microgrid comprises four PVPPs, for which the rated active power (P_{max}), and reactive power limits (Q_{min} and Q_{max}) are presented in Table 3. The negative values for reactive power imply that the inverter absorbs the reactive power from the point of common coupling. It should be mentioned that the Q_{min} and Q_{max} values correspond to a 0.85 power factor at the PVPP rated active power, therefore the PV inverters have the capability to continuously regulate the reactive power absorption or injection between these limits at any given active power output between 0% and 100% of their active rated power.

Table 3

PVPP data

PV	P_{max} [kW]	Q_{min} [kvar]	Q_{max} [kvar]	S_{max} [kVA]
PV2	330	–205	205	388.5
PV3	950	–589	589	1117.8
PV6	350	–217	217	411.8
PV8	1050	–651	651	1235.4

The data corresponding to the three installed capacitor banks are presented in Table 4: a maximum number of steps (n_{CBmax}), rated voltage (U_r) and rated reactive power per step ($Q_{r,step}$). It should also be noted that the capacitor banks are modeled as a constant susceptance for the load flow calculation.

Table 4

Capacitor banks data

CB	n_{CBmax}	Parameters
CB4	5	U_r = 20 kV $Q_{r,step}$ = 100 kvar
CB5	5	
CB7	5	

4.2 SIMULATION ALGORITHM

The simulations presented in this case study are conducted on multiple scenarios by solving the optimization problem formulated in section 2 using the sine-cosine algorithm presented in section 3. All simulations are performed under the MATLAB environment, based on the scripts created by the authors for solving the optimization problem, performing the microgrid load flow calculation using the Backward-Forward Sweep Algorithm and data manipulation. It should be noted that the SCA code utilized in this paper is provided by S. Mirjalili, [16].

Three different scenarios are considered regarding the power demanded by the loads, namely light load (S1), baseload (S2), and heavy load (S3). The base load scenario is defined by the load values given in Table 1. The light load scenario is defined by reducing the active and reactive demanded power by 15 % for all loads, while the heavy load scenario is characterized by a 15% increase in demand power. Five scenarios are defined for the PVPPs output, by applying the PV generation coefficient (P_{PV}) of 0 %, 25 %, 50 %, 75 %, and 100 % on the active rated power P_{max}. Finally, the 15 scenarios, obtained by generating all the possible combinations between the load demand and PV generation scenarios, are presented in Table 5.

Table 5

Considered scenarios

Load \ P_{PV} (%)	0 %	25 %	50 %	75 %	100 %
Light Load	S.1.0	S.1.1	S.1.2	S.1.3	S.1.4
Base Load	S.2.0	S.2.1	S.2.2	S.2.3	S.2.4
Heavy Load	S.3.0	S.3.1	S.3.2	S.3.3	S.3.4

4.3. RESULTS AND DISCUSSIONS

The case study presents the impact of using the PVPPs to inject reactive power upon the microgrid active power losses and voltage profile, for the 15 considered scenarios. For each scenario, a reference strategy is defined by using only the capacitor banks for reactive power management, while the PVPP operates at a unitary power factor. The reference strategy is defined according to the voltage control paradigm that was applied for PVPPs until recently, which stated that "inverters should not actively participate in voltage/var regulation" [23]. Furthermore, the impact of the reactive power support provided by the PVPPs on the microgrid's operating conditions is clearly revealed by comparison to the reference strategy, where no reactive power support is provided. For the reference strategy, the optimal CB operating step is determined by solving a simplified version of the optimization problem formulated in section 2, where only the $x_{CB,1}$, … $x_{CB,n}$ variables are considered. The optimal settings for all scenarios according to the reference strategy are n_{CB4} = 5, n_{CB5} = 5, and n_{CB7} = 5, which represents the maximum available step for all three CBs comprised within the microgrid. Figure 3 presents the bus voltage microgrid's profile for all Base Load scenarios (S.2.0 – S.2.4).

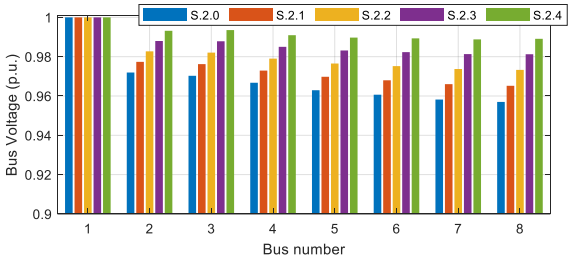

Fig. 3 – Microgrid bus voltage profiles obtained in the base load scenarios, for the reference strategy.

The results presented in Fig. 3 reveal that the bus voltage values are comprised, for all base load scenarios, between 1

p.u and 0.9570 p.u. (at bus 8 in S.2.0). The lowest bus voltage is observed at bus 8 for the first four scenarios, while for the last scenario, where the active power output of the PVPPs is maximum, at bus 7. The minimum bus voltage value is 0.9641 p.u. in the light load scenarios (S.1.0 – S.1.4) and 0.9497 p.u. in the heavy load scenarios (S.3.0 – S.3.4).

Hereinafter, the microgrid operating conditions obtained by applying the proposed strategy, which consists in using the PVPPs to inject reactive power alongside the CBs, are presented in comparison with the reference strategy.

The first part of this section presents the results obtained for one representative scenario, namely S.2.3, defined by Base Load and 75% PV generation. The optimal settings for the PV reactive power output are: Q_{PV2} = 466.71 kvar, Q_{PV3} =197.36 kvar, Q_{PV6} =125.43 kvar, Q_{PV8} = 495.26 kvar while the optimal CB operating steps are n_{CB4} = 3, n_{CB5} =2 and n_{CB7} =3. The microgrid bus voltages are presented in Fig. 4 as a comparison between the values obtained applying the optimal settings provided by the SCA and the values from the reference strategy when the PVPPs operate at a unitary power factor.

The reactive power injected in the two considered strategies is relatively close, as approx. 1589 kvar are injected by both PVPPs and CBs, while in the reference strategy the CBs supplied approx. 1500 kvar. Therefore, the results presented in Fig. 4 reveal a relatively reduced impact of the reactive power support provided by the PVPPs upon the bus voltage profile, as the maximum increase of 0.0011 p.u., is observed at bus 8. In the proposed strategy, the amount of supplied reactive power is close to the value in the reference strategy, but a better distribution of the reactive power sources throughout the microgrid is achieved. Consequently, the active losses are decreasing by 15%, from 28.38 kW to 24.12 kW.

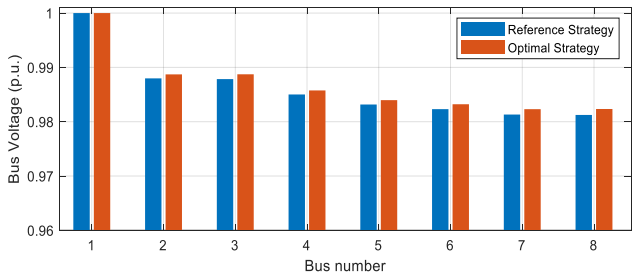

Fig. 4 – Comparison between microgrid bus voltages.

The second part of this section presents a synthesis of the results obtained for the 15 considered scenarios. The optimal reactive power output for the four PVPP is presented in Fig. 5, while the optimal operating step settings for the three CBs are shown in Fig. 6.

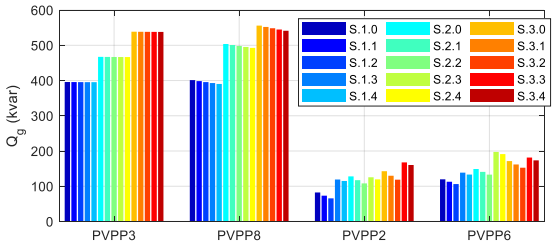

Fig. 5 – PV Inverters optimal reactive power output.

From Fig. 5, it can be observed that the reactive power output for PV3 and PV8 is slightly decreasing as the active power output increases. The step-like variation of the CB reactive power output also influences the PVPP reactive power output. In scenarios S.2.3 and S.2.4 when n_{CB5} is decreased from 3 (in S.2.0 – S.2.2) to 2, the PV6 reactive power output which was slightly decreasing in S.2.0-S.2.2 increases with 65 kvar and then it continues to decrease. Similar behavior is observed for PV2 due to the CB4 step-change in S.3.3. Also, due to the increased load demand in S.3 scenarios, CB7 operating step is increased from 3 (in all S.0 and S.1 scenarios) to 4 (in all S.3 scenarios).

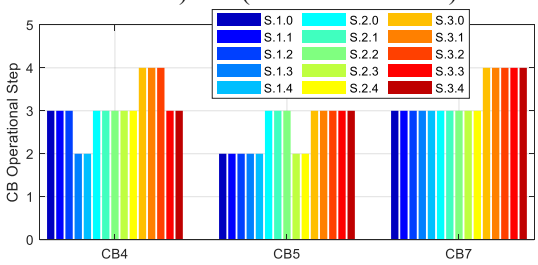

Fig. 6 – Capacitor banks optimal step settings.

Figure 7 presents the minimum (U_{min}) and average (U_{avg}) bus voltage values for both reference and optimal strategies in all the 15 considered scenarios. The results reveal that the impact on bus voltage is increasing as the load increases. For example, in the S.3.1 scenario (heavy load and P_{PV} = 25%), both minimum and average bus voltage values are increased by 0.002 p.u., while for the light load scenarios the increase is even lower.

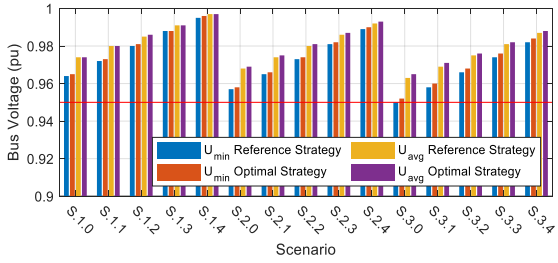

Fig. 7 – Minimum and average voltage.

As expected, the impact of the PVPP reactive power injection upon the microgrid voltage profile is reduced, as the reactive power injected by the CBs in the reference strategy of about 1500 kvar, is replaced by a total reactive power between 1700 kvar (in light-load scenarios) and 2500 kvar (in heavy load scenarios) injected by both PVPPs and CBs. Although the reactive power injection is better to spread throughout the microgrid and PVPPs offer continuous reactive power control, the microgrid reactive power support provided by the CBs during light load conditions is relatively close to the optimal solution. Furthermore, the voltage sensibility to reactive power variation is relatively reduced, due to the reduced *X*/*R* ratio that is specific to MV networks.

The active power loss reduction is presented in Fig. 8, expressed in percentage relative to the reference strategy. The blue bars represent the light load scenarios, the base load scenarios are represented by the red bars and the heavy load by yellow bars. The bars are grouped within the figure by the PVPP active power output P_{PV}, expressed in percentage relative to the active rated power P_{max}.

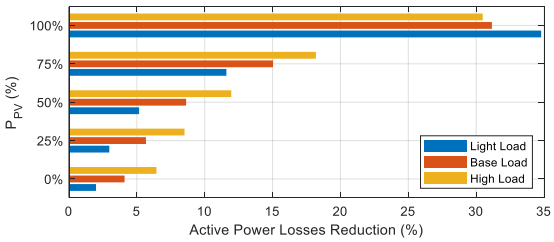

Fig. 8 – Active power losses reduction.

The results presented in Fig. 8 reveal a considerable impact of the PVPPs reactive power injection upon the active power losses. In the light load scenarios, the active power losses are reduced by at least 2% (for P_{PV} = 0%) and up to 34.8% (for P_{PV} = 100%). For the heavy load scenarios, the PVPP reactive power support reduces active power losses by at least 6.4% (for P_{PV} = 0%) and up to 30.5% (at P_{PV} = 100%). The active power loss reduction is achieved by the PVPPs continuous reactive power support as compared to the step-like variation of the CBs reactive power output and a better distribution of the reactive power sources throughout the microgrid. On the other hand, in higher load scenarios, the optimal necessary reactive power exceeds the CBs capacity of 1500 kvar.

5. CONCLUSIONS

The study presented in this paper aims to integrate the reactive power generated by the PVPPs inverters in providing an optimal reactive power management strategy for minimizing the active power losses of a microgrid. The optimization problem formulated in section 2 is solved by using the sine-cosine algorithm for 15 scenarios defined by generating all possible combinations between the light, base, and heavy load and 0%, 25%, 50%, 75% and 100% PVPP active power output.

The microgrid reactive power management strategy consists in simultaneously controlling the capacitor banks' operating steps and the reactive power generated by the PVPPs inverters. A reference reactive power management strategy is also considered as a term of comparison, where all PVPPs inverters operate at unitary power factor and only the capacitor banks are used for providing reactive power support. The results show that, although the bus voltage profile is slightly improved, the total microgrid active power losses are reduced by a significant amount. Moreover, active power losses are also reduced when the PVPP inverters are only used for providing reactive power support, without generating active power. In conclusion, this study demonstrates that the PVPP inverters are effective in reducing the active power losses in microgrids by providing reactive power support.

Received on 11 November 2021.

REFERENCES

1. Sk.A. Aleem, S.M.S. Hussain, T.S. Ustun, *A review of strategies to increase PV penetration level and impact of PV penetration on grid*, Energies, **13**, *3*, pp. 636 (2020).
2. IEEE Std 2030.7-2017, *IEEE Standard for the Specification of Microgrid Controllers*
3. A.C. Pérez-Flores, J.D.M. Antonio, V.H. Olivares-Peregrino, H. R. Jiménez-Grajales, A. Claudio-Sánchez, G. V. G. Ramírez, *Microgrid energy management with asynchronous decentralized particle swarm optimization*, IEEE Access, **9**, pp. 69588-69600 (2021).
4. N. Sridhar, M. Kowsalya, *Enhancement of power management in micro grid system using adaptive ALO technique*, Journal of Ambient Intelligence and Humanized Computing, **12**, pp. 2163–2182 (2021)
5. K.S. Nimma, M.D.A Al-Falahi, H.D. Nguyen, S.D.G Jayasinghe, T.S. Mahmoud, M. Negnevitsky, *Grey wolf optimization-based optimum energy-management and battery-sizing method for grid-connected microgrids*, Energies, **11**, *4*, pp. 847 (2018)
6. D. Sidea, L. Toma, M. Sanduleac, I. Picioroaga, V. Boicea, *Optimal BESS scheduling strategy in microgrids based on genetic algorithms*, 2019 IEEE Milan PowerTech, Milan, Italy, 2019
7. Y.O. Shaker, D. Yousri, A. Osama, A. Al-Gindy, E. Tag-Eldin D. Allam, *Optimal charging/discharging decision of energy storage community in grid-connected microgrid using multi-objective hunger game search optimizer*, IEEE Access, **9**, pp. 120774-120794 (2021)
8. W. Al-Saedi, S. Lachowicz, D. Habibi, O. Bass, *Power quality enhancement in autonomous microgrid operation using Particle Swarm Optimization*, International Journal of Electrical Power & Energy System, **42**, *1*, pp. 1-6 (2011)
9. D.O. Sidea, I.I. Picioroaga, C. Bulac, *Optimal battery energy storage system scheduling based on mutation-improved grey wolf optimizer using GPU-accelerated load flow in active distribution networks*, IEEE Access, **9**, pp. 13922-13937, (2021)
10. S.A. El-sattar, S. Kamel, M. Ebeed, F. Jurado, *An improved version of salp swarm algorithm for solving optimal power flow problem*. Soft Computing, **25**, pp. 4027-4052 (2021)
11. M. Moradian, A. Najjar-Khodabakhsh, S. Shojaeian, *Unit commitment cost and reliability optimization based on an improved genetic algorithm,* Rev. Roum. Sci. Techn. – Électrotechn. Et Énerg., **59**, *1*, pp. 25-33 (2014)
12. H. Labdelaoui, F. Boudjema, D. Boukhetala, *Multiobjective Optimal Design of Dual-Input Power System Stabilizer using Genetic Algorithms,* Rev. Roum. Sci. Techn. – Électrotechn. Et Énerg., **62**, *1*, pp. 93-97 (2017).
13. S. Ziane, A. Abdelghani, M. Abid, *Power control of doubly fed induction generator using hybrid adaptive neural fuzzy sliding mode controller optimised by genetic algorithm,* Rev. Roum. Sci. Techn. – Électrotechn. Et Énerg., **63**, *4*, pp. 411-416 (2018).
14. M. Eremia (ed.) *et al. - Electric Power Systems: Vol. 1 Electric networks*, Publishing House of the Romanian Academy, Bucharest (2006).
15. C.T. Phan-Tan, M. Hill, *Optimal PV inverter control for network voltage and power factor regulation*, 2020 IEEE 11th International Symposium on Power Electronics for Distributed Generation Systems (PEDG) (2020).
16. S. Mirjalili, *SCA: A Sine Cosine Algorithm for Solving Optimization Problems*, Knowledge-Based Systems, **96**, pp. 120-133 (2016).
17. A.B. Gabis, Y. Meraihi, S. Mirjalili, A. Ramdane-Cherif, *A comprehensive survey of sine cosine algorithm: variants and applications*, Artificial Intelligence Review, **54**, pp. 5469-5540 (2021).
18. D. Gonidakis , A. Vlachos, *A new sine cosine algorithm for economic and emission dispatch problems with price penalty factors*, Journal of Information and Optimization Sciences, **40**, *3*, pp. 679–697 (2019).
19. R.K. Sahu, B. Shaw, J.R. Nayak, *Fractional-order PID controller optimized by SCA for solar system*, International Conference on Artificial Intelligence, Smart Grid and Smart City Applications, Springer, pp. 1–10 (2019).
20. A. A. Abdelsalam, *Optimal distributed energy resources allocation for enriching reliability and economic benefits using sine–cosine algorithm*, Technology and Economics of Smart Grids and Sustainable Energy, **5**, *1*, pp. 1–18 (2020).
21. *TF C6.04.02: TB 575 Benchmark Systems for Network Integration of Renewable and Distributed Energy Resources*, CIGRE, 2014
22. Twenpower Medium-Voltage XLPE Cables Catalogue, on-line at: https://t3.lappcdn.com/fileadmin/DAM/Miltronic_Sweden/4_Servicecenter/2Nedladdningscenter/TKF_Twenpower_Medium_Voltage.pdf
23. M. Farivar, R. Neal, C. Clarke, S Low, *Optimal Inverter VAR Control in Distribution Systems with High PV Penetration*, 2012 IEEE Power and Energy Society General Meeting, San Diego, USA, (2012).